Bose-Einstein condensation with internal degrees of freedom

Masahito Ueda

Tokyo Institute of Technology

Group members

Tokyo Tech (theory): spinor, dipolar, mixture gases

M. Ueda

H. Saito (spinor BEC)

Y. Kawaguchi (dipolar BEC) → poster (P-27)

D. Roberts (degenerate mixture)

Gakushuin (experiment): spinor, mixture gases

T. Hirano

T. Kuwamoto

→ collaborative project (theory + experiment)

focus on BECs with internal degrees of freedom

Contents

- Atomic-gas BECs vs. superfluid helium

- Spin-1 and Spin-2 BECs

  - ground-state phase diagram
  - many-body effects
  - spin-exchange dynamics
  - spontaneous symmetry breaking and pattern formation of spin textures

Atomic-gas BECs vs. Superfluid helium

Atomic-gas BECs vs. Superfluid helium

↓

striking complementarity in many respects

	Superfluid helium	Atomic-gas BEC
Phase	liquid →imcompressible	gas → highly compressible → highly susceptible to external perturbations
Detection of BEC	realized using neutron scattering but not straightforward	straightforward using time-of-flight measurement
Microscopic understanding of the container	difficult (microscopic roughness) The container acts as a thermal reservoir.	possible (electromagnetic trap with no microscopic roughness) The container acts as a potential.
Detection of superfluidity	straightforward The Hess-Firbank effect and persistent current offer two hallmarks of superfluidity.	not straightforward Even the normal component can flow permanently once it is set into motion .

	Superfluid helium	Atomic-gas BEC
Kinetics	collision time collective mode $\tau_{col} \sim 10^{-12} s << \omega^{-1}$ ↓ • local equilibrium ensured • physics can be understood by conservation laws (energy, continuity equation, etc.) and hydrodynamics	$\tau_{col} \sim 10^{-3} s \sim \omega^{-1}$ ↓ • not local equilibrium (Knudsen regime) • nonequilibrium relaxation and kinetics essential for BEC phase transition and vortex nucleation 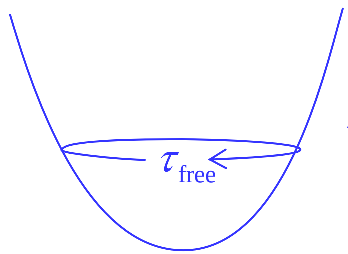 $\tau_{free} < \tau_{col}$
Magnetic moment Internal degrees of freedom	nuclear spin (^3He)	electronic spin : BEC vs. magnetism • local control of spin texture • new phase such as cyclic phase
Symmetry breaking	• thermodynamic limit ensured • spontaneous symmetry breaking of relative gauge ↓ emergence of mean field	mesoscopic (not thermodynamic limit) ↓ • symmetry breaking not necessarily occur • fragmented BECs

Spin-2 BEC

$$2 \otimes 2 = 0 \oplus 2 \oplus 4 \oplus \underbrace{1 \oplus 3}$$

a_0 a_2 a_4 forbidden by Bose symmetry

Koashi & Ueda, PRL 84, 1066 (2000)
Ciobanu, et al., PRA 61,033607 (2000)
Ueda & Koashi., PRA 65, 063602 (2002)

Interaction Hamiltonian

$$\hat{V} = \frac{1}{2}\int d\mathbf{r}\left[c_0 :\hat{n}^2: + c_1 :\hat{\mathbf{F}}^2: + c_2 \hat{S}^\dagger \hat{S}\right]$$

$$c_0 \sim 4a_2 + 3a_4$$
$$c_1 \sim a_4 - a_2$$
$$c_2 \sim 7a_0 - 10a_2 + 3a_4$$

$\hat{n} = \sum_m \hat{\psi}_m^\dagger \hat{\psi}_m$ $\cdots$ particle density

$\hat{\mathbf{F}} = \sum_m \hat{\psi}_m^\dagger \mathbf{f}_{mn} \hat{\psi}_n$ $\cdots$ spin density

$\hat{S} = \sum_m \frac{(-1)^m}{\sqrt{5}} \hat{\psi}_m \hat{\psi}_{-m}$ $\cdots$ spin-singlet pair amplitude

FM ^{83}Rb, ^{87}Rb$(f=1)$

AFM ^{87}Rb$(f=2)$, ^{23}Na $(f=1, 2)$

cyclic ^{85}Rb$(?)$

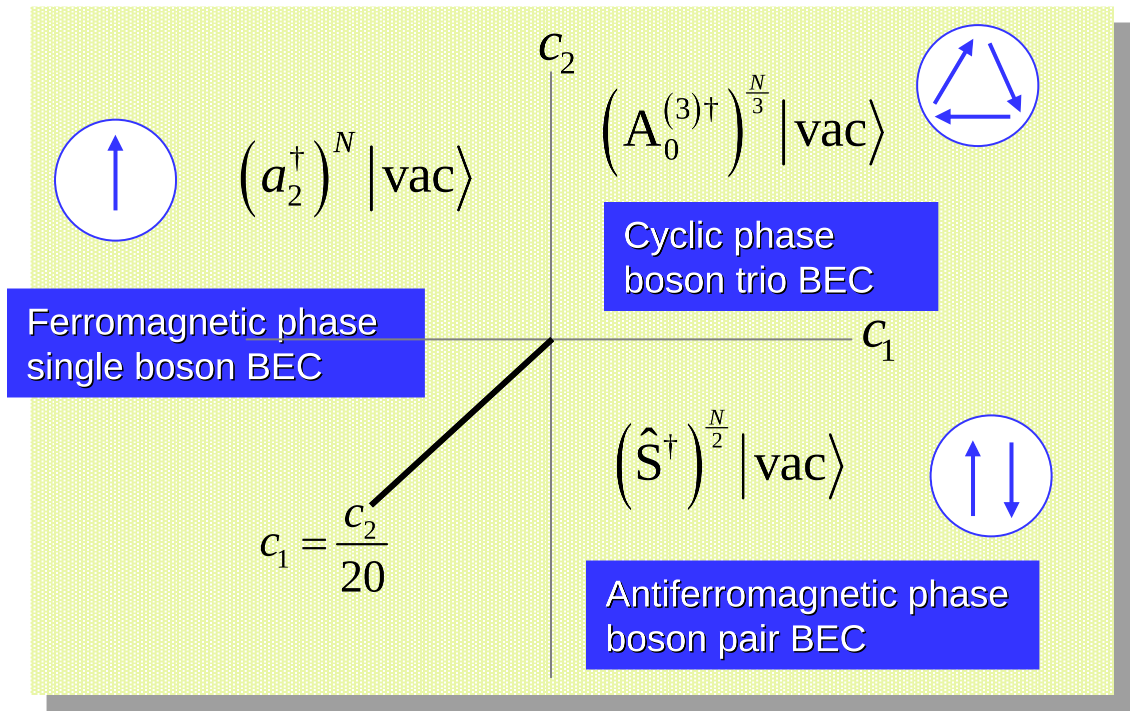

“ Meissner Effect ” of the Antiferromagnetic Spin-2 BEC

Spin-dependant part of the Hamiltonian

$$\hat{H}^{\rm spin} = \frac{c_1}{2V^{\rm eff}} : \hat{\mathbf{F}}^2 : + \frac{2c_2}{5V^{\rm eff}} \hat{S}^\dagger \hat{S} - \underbrace{p\hat{F}_z}_{\text{Zeeman term}} \qquad p = g\mu B \qquad \left| N, N_s, F, F_z; \lambda \right\rangle$$

# of spin-single pairs

Minimize the eigenergy with respect to F2

external magnetic field

screening field

$$E(F_z, l) = \frac{c_1'}{2V^{\rm eff}} \left[F_z - \frac{V^{\rm eff}}{c_1'} \left(p - \frac{|c_2|}{8V^{\rm eff}} \right) + \frac{1}{2} \right]^2 - \frac{c_2}{40V^{\rm eff}} l(l + 2F + 6) + \text{const.}$$

Mesoscopic effect

$$c_1' \equiv \tfrac{1}{V^{\rm eff}} \left(c_1 - \tfrac{c_2}{20} \right)$$

$$l = 2(N - 2N_s) - F_z$$

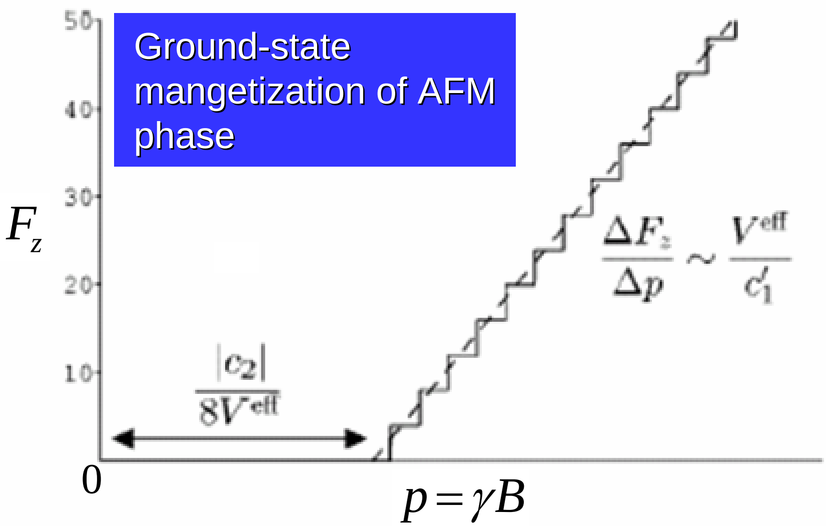

Screening effect of the external magnetic field due to the spin-single pair formation (mesoscopic effect)

Ueda & Koashi, Phys. Rev. A **65**, 063602 (2002)

Ferromagnetism vs. Spin Conservation

How does spontaneous magnetization of a ferromagnet occur in an isolated system in which the total spin angular momentum is conserved ?

Ferromagnetism vs. Spin Conservation

How does spontaneous magnetization of a ferromagnet occur in an isolated system in which the total spin angular momentum is conserved ?

⬇

The system develops local magnetic domains of various types, which depend on the geometry of the trapping potential.

Spin Dynamics in a Cigar-Shaped Trap

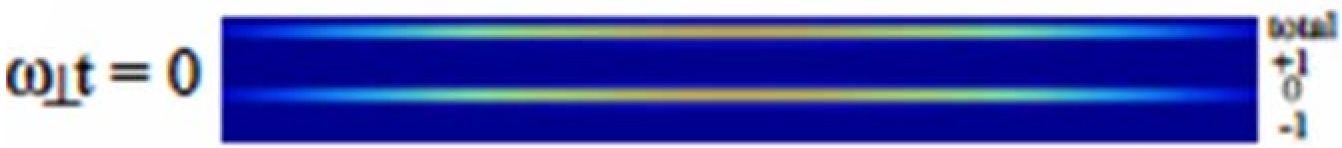

initial state

$$\psi_1 = 0$$

$$\psi_0 = \sqrt{1 - 10^{-4}}\,\psi_g$$

$$\psi_{-1} = 0.01\psi_g$$

H.Saito and M.Ueda, Phys. Rev. A**72**, 023610 (2005)

Spin Dynamics in a Cigar-Shaped Trap

initial state

$$\psi_1 = 0$$
$$\psi_0 = \sqrt{1-10^{-4}}\psi_g$$
$$\psi_{-1} = 0.01\psi_g$$

Observed by
Gakushuin group!

H.Saito and M.Ueda, Phys. Rev. A**72**, 023610 (2005)

Spin Dynamics in a Cigar-Shaped Trap

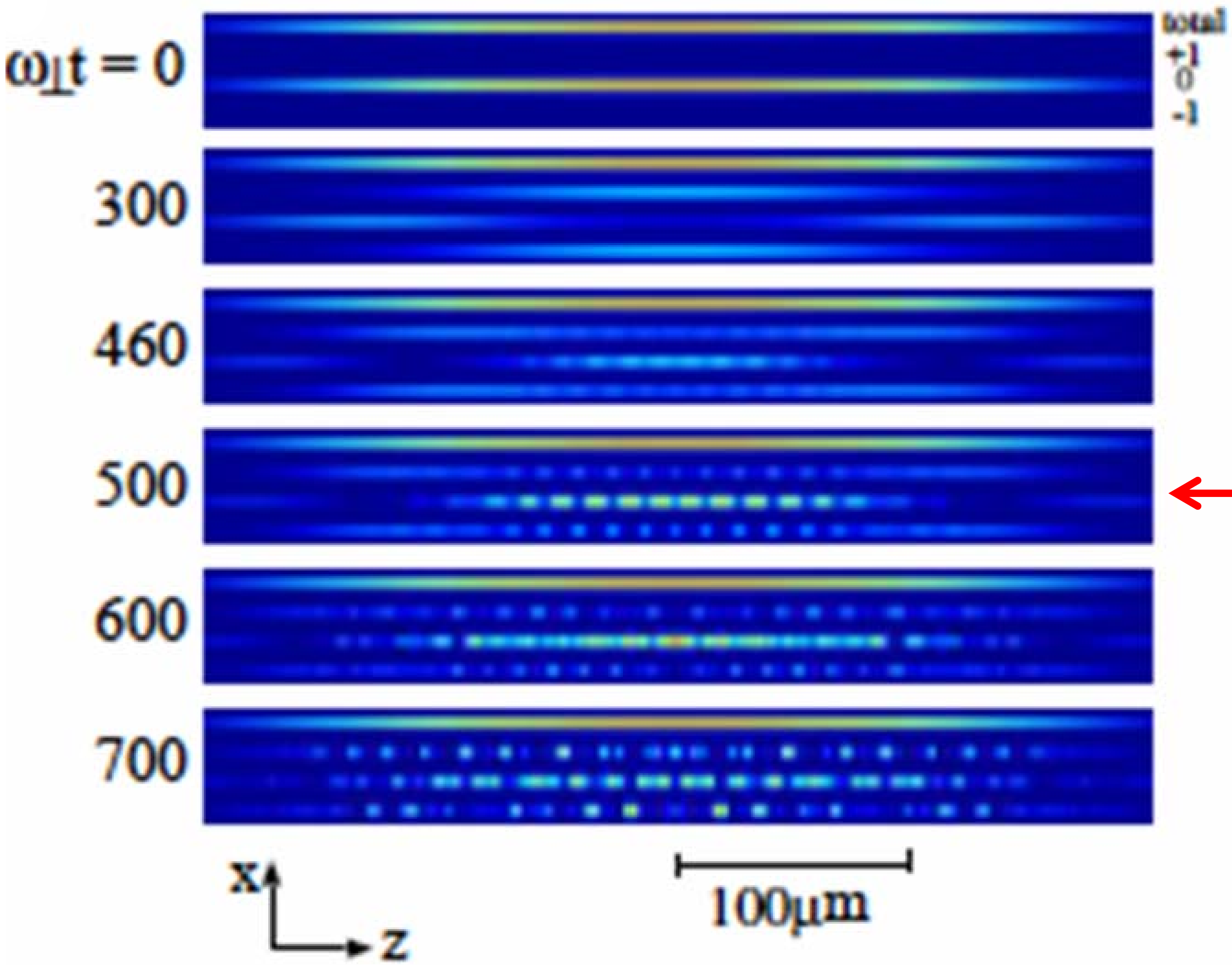

initial state

$$\psi_1 = 0$$

$$\psi_0 = \sqrt{1-10^{-4}}\,\psi_g$$

$$\psi_{-1} = 0.01\psi_g$$

modulational instability

H.Saito and M.Ueda, Phys. Rev. A**72**, 023610 (2005)

Mean Spin Vector along the Trap Axis (r =0)

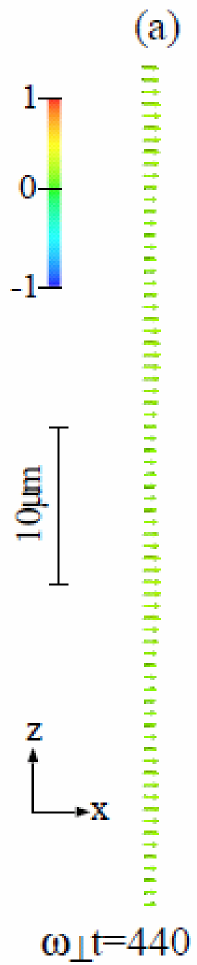

FIG. 3: The mean spin vectors $\boldsymbol{F}/n$ at $r = 0$ seen from the $-y$ direction, where the vertical axis is the z axis. The conditions are the same as those given in Fig. 1. The length of the spin vector is proportional to $|\boldsymbol{F}|/n$, and the color represents F_z/n according to the gauge shown at the top left corner. The spin vector is displayed from $z = 0$ to $z = 54\mu$m in (a)-(c), and from $z = 35\mu$m to $z = 89\mu$m in (d). The Larmor precession in the x-y plane is eliminated for clarity of presentation.

Mean Spin Vector at r =0

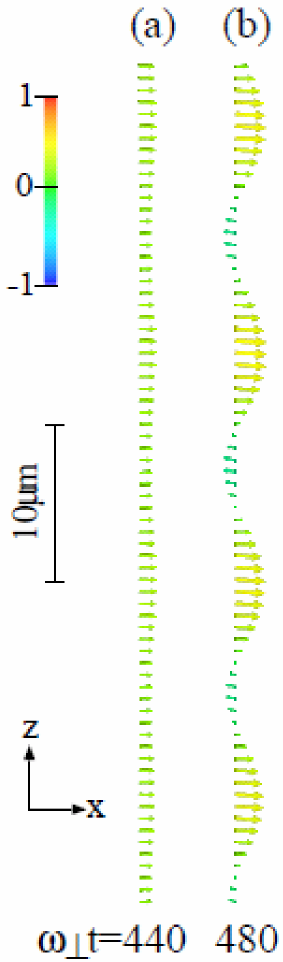

FIG. 3: The mean spin vectors $\boldsymbol{F}/n$ at $r = 0$ seen from the $-y$ direction, where the vertical axis is the z axis. The conditions are the same as those given in Fig. 1. The length of the spin vector is proportional to $|\boldsymbol{F}|/n$, and the color represents F_z/n according to the gauge shown at the top left corner. The spin vector is displayed from $z = 0$ to $z = 54\mu$m in (a)-(c), and from $z = 35\mu$m to $z = 89\mu$m in (d). The Larmor precession in the x-y plane is eliminated for clarity of presentation.

The staggeed magnetic domains grow during $\omega \perp t = 440 \sim 520$

Mean Spin Vector at r =0

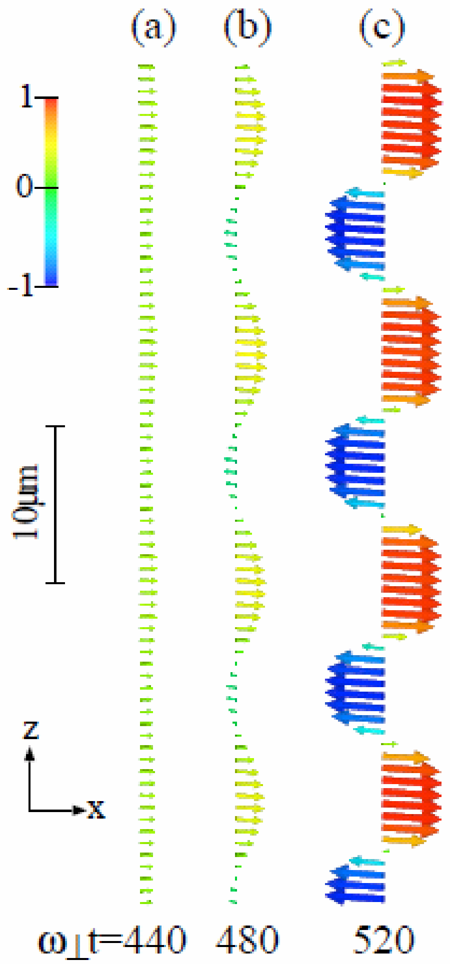

FIG. 3: The mean spin vectors $\boldsymbol{F}/n$ at $r = 0$ seen from the $-y$ direction, where the vertical axis is the z axis. The conditions are the same as those given in Fig. 1. The length of the spin vector is proportional to $|\boldsymbol{F}|/n$, and the color represents F_x/n according to the gauge shown at the top left corner. The spin vector is displayed from $z = 0$ to $z = 54\mu$m in (a)-(c), and from $z = 35\mu$m to $z = 89\mu$m in (d). The Larmor precession in the x-y plane is eliminated for clarity of presentation.

The staggeed magnetic domains grow during $\omega \perp t = 440 \sim 520$

Mean Spin Vector at r =0

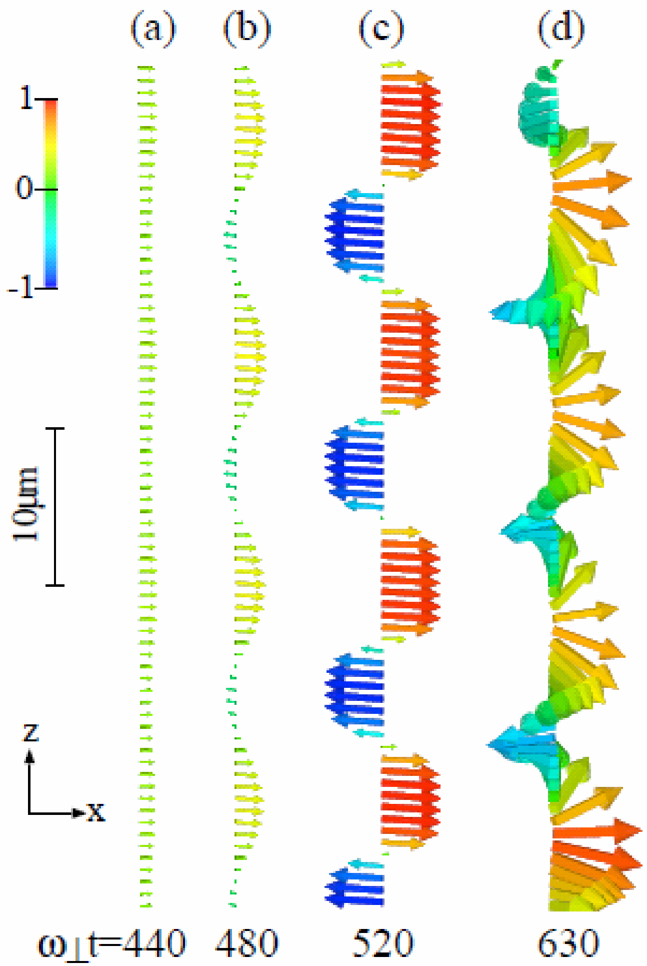

FIG. 3: The mean spin vectors $\boldsymbol{F}/n$ at $r = 0$ seen from the $-y$ direction, where the vertical axis is the z axis. The conditions are the same as those given in Fig. 1. The length of the spin vector is proportional to $|\boldsymbol{F}|/n$, and the color represents F_z/n according to the gauge shown at the top left corner. The spin vector is displayed from $z = 0$ to $z = 54\mu$m in (a)-(c), and from $z = 35\mu$m to $z = 89\mu$m in (d). The Larmor precession in the x-y plane is eliminated for clarity of presentation.

The staggeed magnetic domains grow during $\omega \perp t = 440 \sim 520$

Helical Structures are spontaneously formed at $\omega \perp t = \sim 630$

Spin Dynamics in a Pancake-Shaped Trap

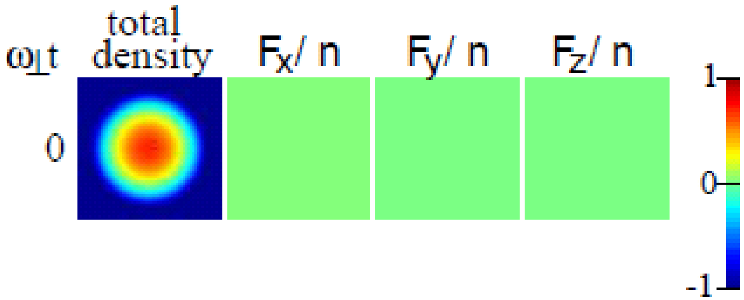

initial state

$$\psi_1 = 0$$
$$\psi_0 = \sqrt{1-10^{-4}}\psi_g$$
$$\psi_1 = 0.01\psi_g$$

FIG. 4: The total density and the three components of the mean spin vector $\boldsymbol{F}/n$ of the two-dimensional system (from left to right panel), where the abscissa and ordinate refer to the x and y coordinates in real space. The size of each image is 48×48 in units of $(\hbar/m\omega_\perp)^{1/2}$. The color for the mean spin vector refers to the gauge. The bottom panel illustrates the direction of the spin at $\omega_\perp t = 26$, where the color represents F_z/n as shown in Fig. 3. The Larmor precession in the x-y plane is eliminated.

Spin Dynamics in a Pancake-Shaped Trap

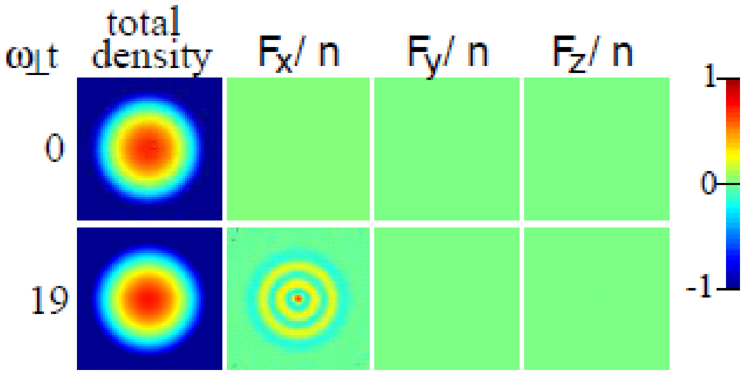

initial state

$$\psi_1 = 0$$
$$\psi_0 = \sqrt{1-10^{-4}}\,\psi_g$$
$$\psi_1 = 0.01\psi_g$$

The concentric ring structure of the spin arises from the dynamical instability.

FIG. 4: The total density and the three components of the mean spin vector $\boldsymbol{F}/n$ of the two-dimensional system (from left to right panel), where the abscissa and ordinate refer to the x and y coordinates in real space. The size of each image is 48×48 in units of $(\hbar/m\omega_\perp)^{1/2}$. The color for the mean spin vector refers to the gauge. The bottom panel illustrates the direction of the spin at $\omega_\perp t = 26$, where the color represents F_z/n as shown in Fig. 3. The Larmor precession in the x-y plane is eliminated.

Spin Dynamics in a Pancake-Shaped Trap

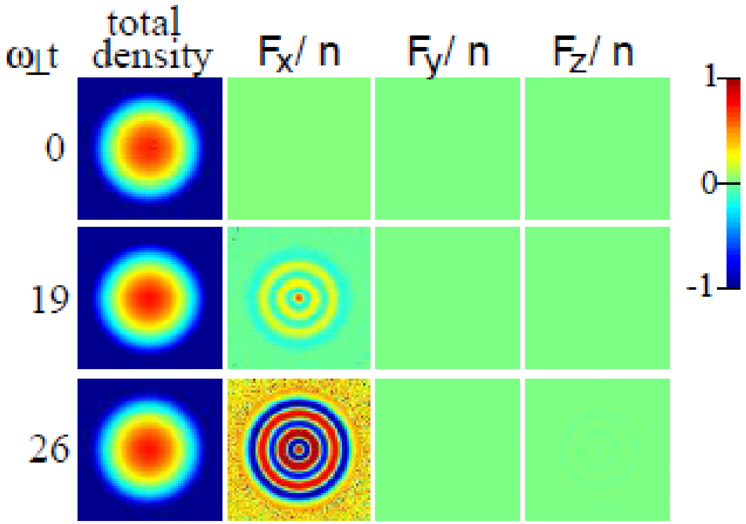

initial state

$$\psi_1 = 0$$
$$\psi_0 = \sqrt{1-10^{-4}}\,\psi_g$$
$$\psi_1 = 0.01\psi_g$$

The concentric ring structure of the spin arises from the dynamical instability.

FIG. 4: The total density and the three components of the mean spin vector $\boldsymbol{F}/n$ of the two-dimensional system (from left to right panel), where the abscissa and ordinate refer to the x and y coordinates in real space. The size of each image is 48×48 in units of $(\hbar/m\omega_\perp)^{1/2}$. The color for the mean spin vector refers to the gauge. The bottom panel illustrates the direction of the spin at $\omega_\perp t = 26$, where the color represents F_z/n as shown in Fig. 3. The Larmor precession in the x-y plane is eliminated.

Spin Dynamics in a Pancake-Shaped Trap

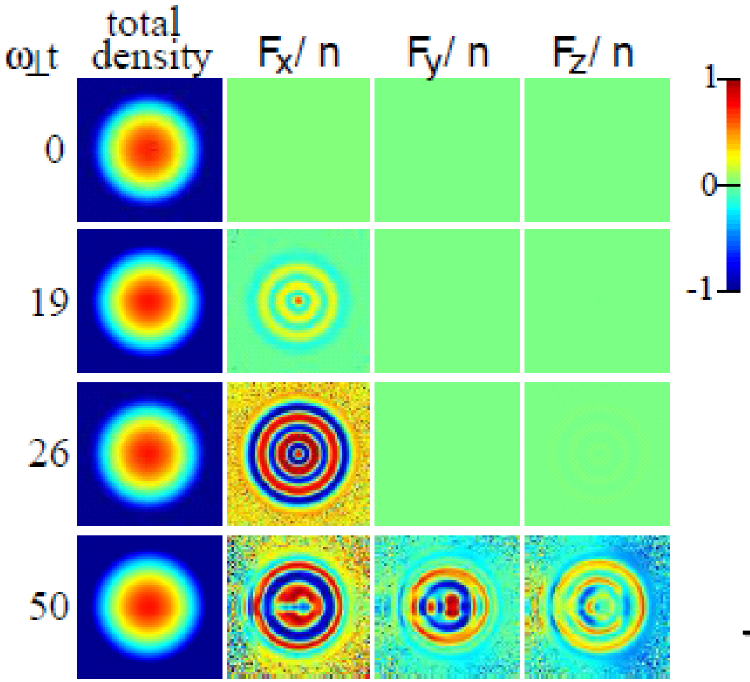

initial state

$$\psi_1 = 0$$
$$\psi_0 = \sqrt{1-10^{-4}}\,\psi_g$$
$$\psi_1 = 0.01\psi_g$$

The concentric ring structure of the spin arises from the dynamical instability.

FIG. 4: The total density and the three components of the mean spin vector $\boldsymbol{F}/n$ of the two-dimensional system (from left to right panel), where the abscissa and ordinate refer to the x and y coordinates in real space. The size of each image is 48×48 in units of $(\hbar/m\omega_\perp)^{1/2}$. The color for the mean spin vector refers to the gauge. The bottom panel illustrates the direction of the spin at $\omega_\perp t = 26$, where the color represents F_z/n as shown in Fig. 3. The Larmor precession in the x-y plane is eliminated.

Spin Dynamics in a Pancake-Shaped Trap

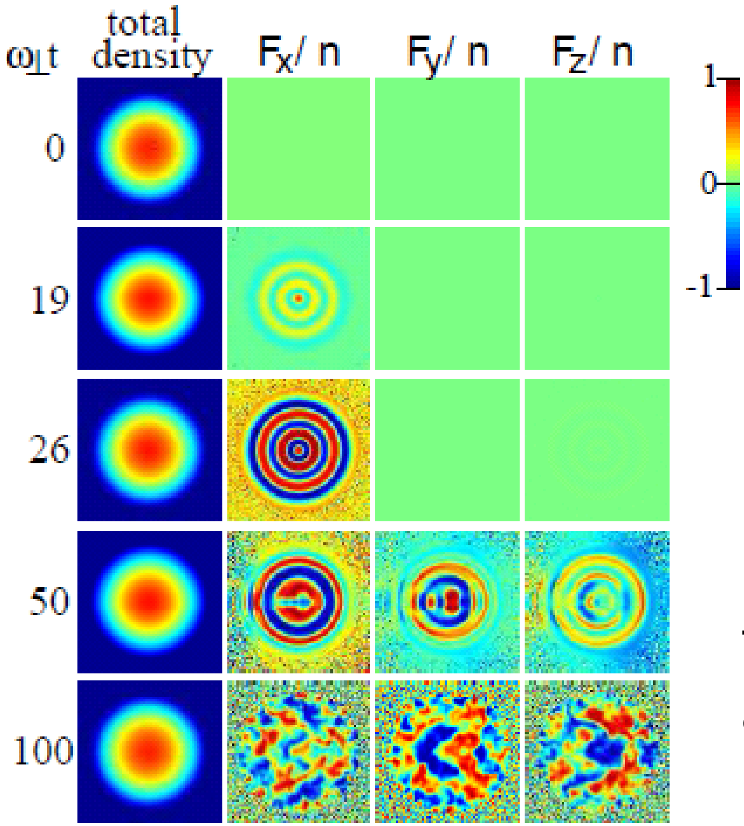

initial state

$$\psi_1 = 0$$
$$\psi_0 = \sqrt{1-10^{-4}}\,\psi_g$$
$$\psi_1 = 0.01\psi_g$$

The concentric ring structure of the spin arises from the dynamical instability.

FIG. 4: The total density and the three components of the mean spin vector $\boldsymbol{F}/n$ of the two-dimensional system (from left to right panel), where the abscissa and ordinate refer to the x and y coordinates in real space. The size of each image is 48×48 in units of $(\hbar/m\omega_\perp)^{1/2}$. The color for the mean spin vector refers to the gauge. The bottom panel illustrates the direction of the spin at $\omega_\perp t = 26$, where the color represents F_z/n as shown in Fig. 3. The Larmor precession in the x-y plane is eliminated.

Spin Dynamics in a Pancake-Shaped Trap

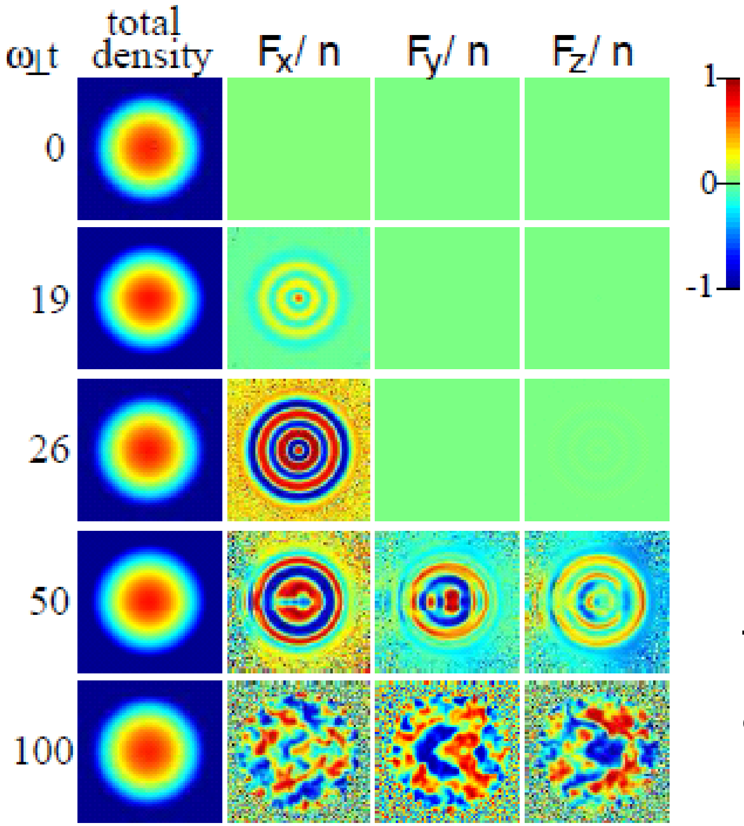

initial state

$$\psi_1 = 0$$
$$\psi_0 = \sqrt{1-10^{-4}}\psi_g$$
$$\psi_1 = 0.01\psi_g$$

The concentric ring structure of the spin arises from the dynamical instability.

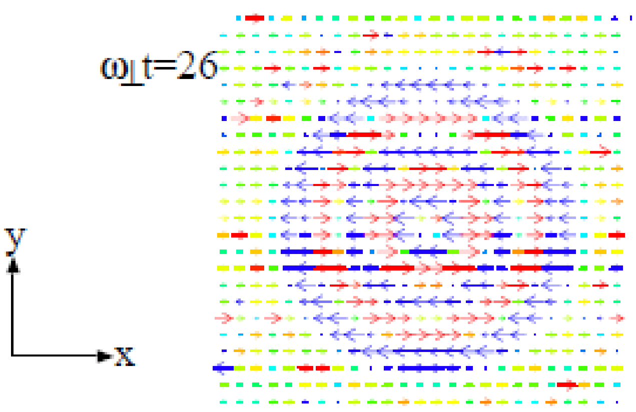

FIG. 4: The total density and the three components of the mean spin vector $\boldsymbol{F}/n$ of the two-dimensional system (from left to right panel), where the abscissa and ordinate refer to the x and y coordinates in real space. The size of each image is 48×48 in units of $(\hbar/m\omega_\perp)^{1/2}$. The color for the mean spin vector refers to the gauge. The bottom panel illustrates the direction of the spin at $\omega_\perp t = 26$, where the color represents F_z/n as shown in Fig. 3. The Larmor precession in the x-y plane is eliminated.

Spin-exchange dynamics: f=2

Spin-Exchange Dynamics (f =2)

H.Schmaljohann, et al., PRL**92**, 040402 (2004)

$$(m=0)+(m=0)\leftrightarrow(m=1)+(m=-1)\leftrightarrow(m=2)+(m=-2)$$

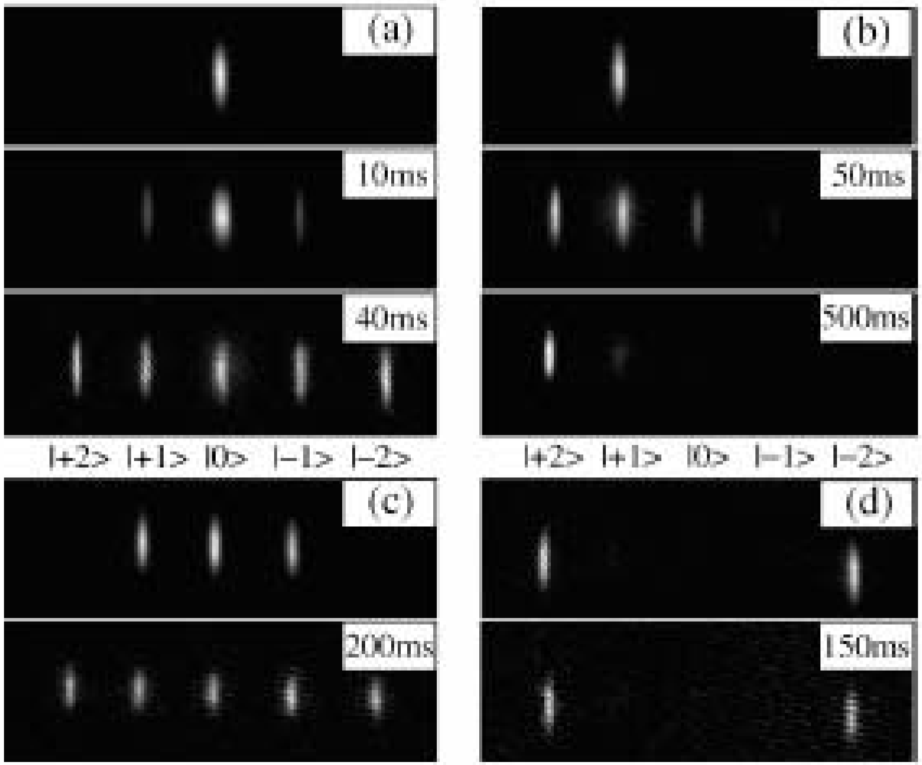

FIG. 1. Time-dependent observation of different m_F components starting from the initially prepared states denoted by (a)–(d). Shown are spinor condensates separated by a Stern-Gerlach method (time of flight 31 ms).

Is the ground state antiferromagnetic or cyclic ?

Spin-Exchange Dynamics (f =2)

T. Kuwamoto, et al., PRA **69**, 063604 (2004)

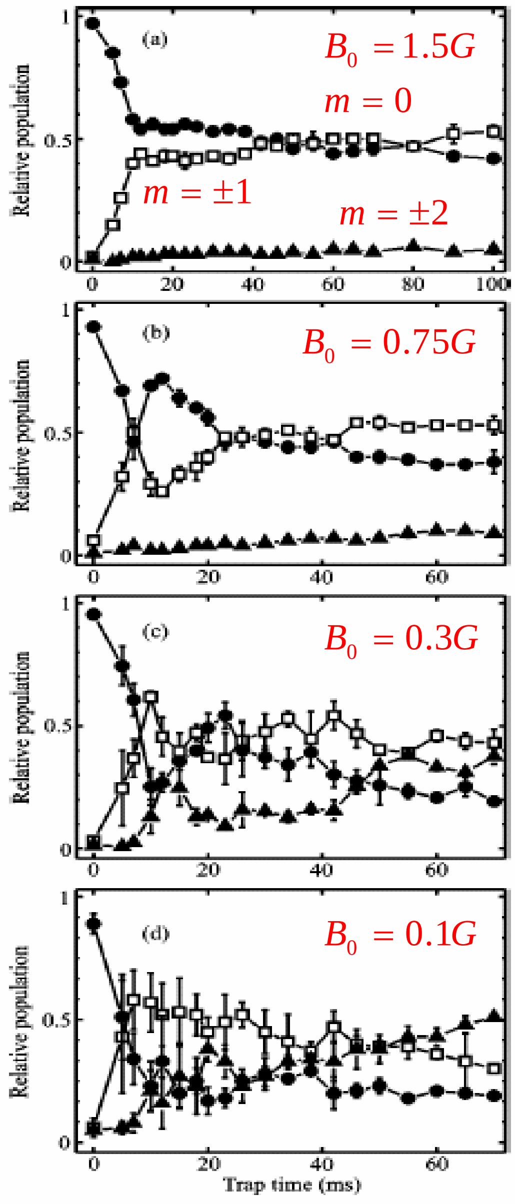

The spin-exchange oscillations last for longer times for lower bias magnetic fields.

Why do the oscillations stop for large magnetic field?

Domain Formation via Spin Exchange (f=2)

H. Saito and M. Ueda, Phys.Rev. A **72**, 053628 (2005)
cond-mat /0504398

experiment | theory

B=0.1G

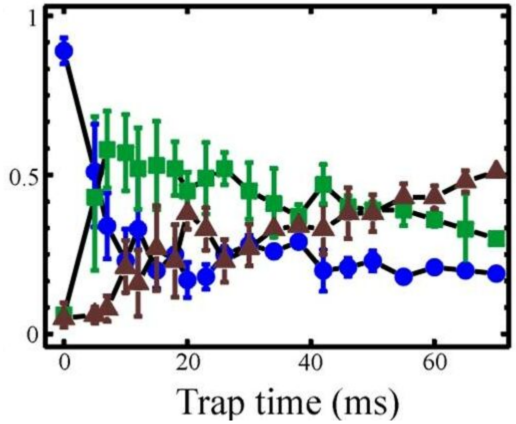

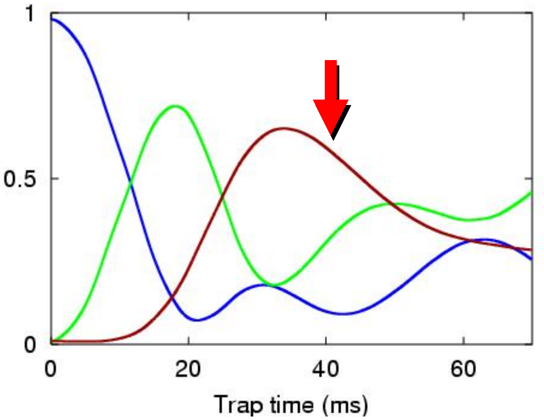

B=1.5G

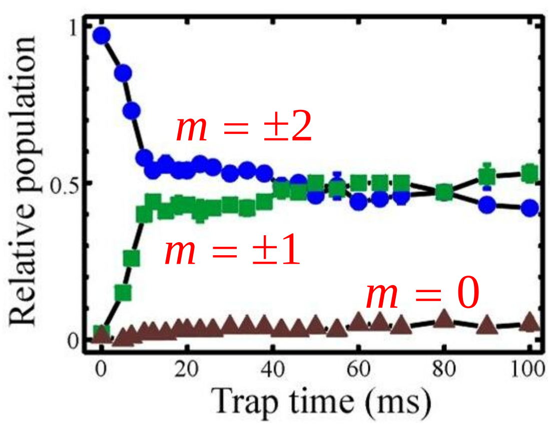

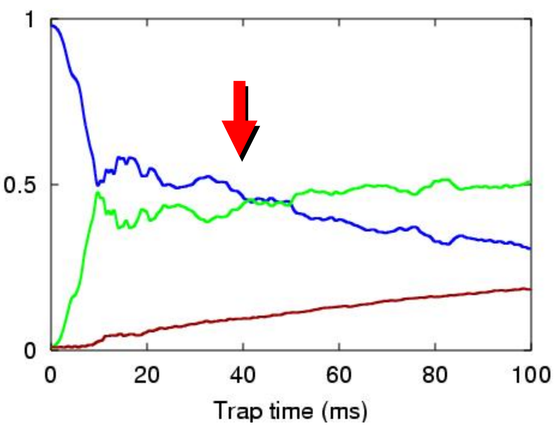

Domain Formation via Spin Exchange (f=2)

H. Saito and M. Ueda, to appear in PRA (2005)
cond-mat /0504398

experiment

theory

total -2 -1 0 1 2

B=0.1G

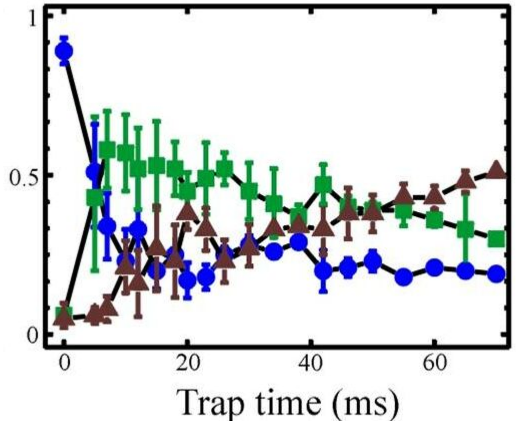

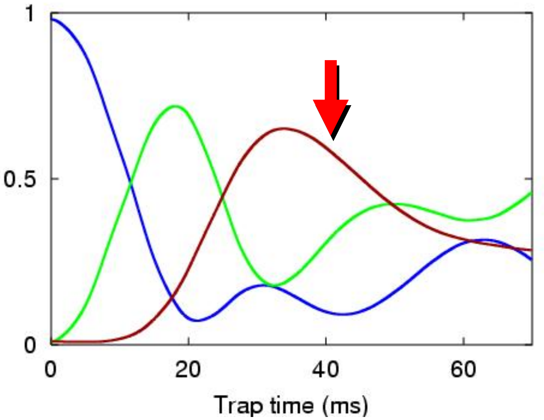

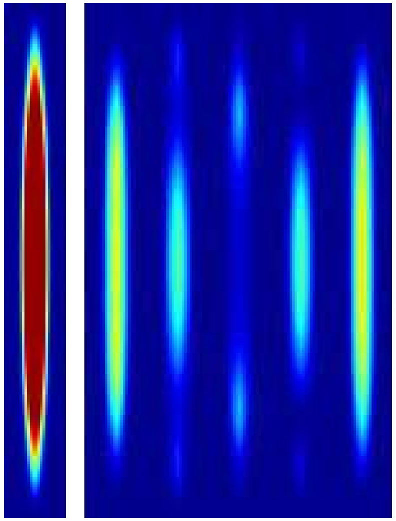

B=1.5G

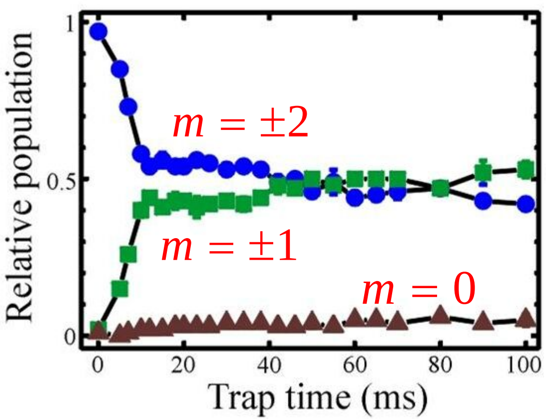

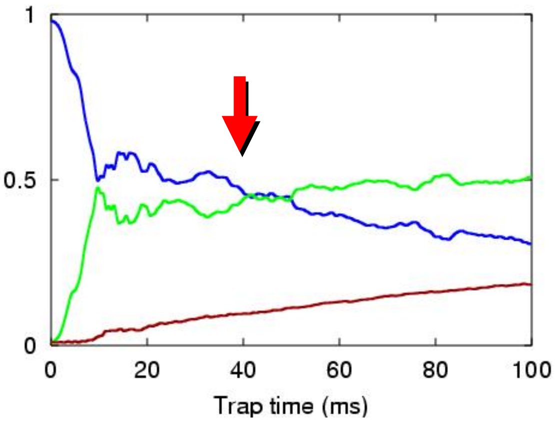

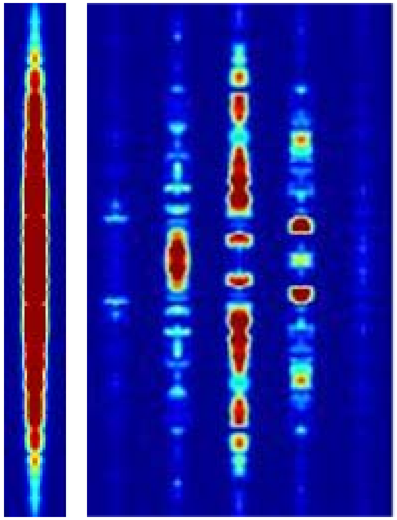

Diagnostics of the ground state phase of a f=2 ^{87}Rb BEC

Diagnostics of the ground state phase of a f=2 ^{87}Rb BEC

- The lifetime of the f=2 ^{87}Rb BEC is relatively long (~100ms) due to a fortuitous coincidence of the singlet and triplet scattering lengths

P. Julienne, et al., Phys. Rev.Lett. **78**, 1880 (1997)

— long enough for coherent spin dynamics to be observed.

— too short for the equilibrium spin state to be achieved (a few seconds required).

Diagnostics of the ground state phase of a f=2 ^{87}Rb BEC

- The lifetime of the f=2 ^{87}Rb BEC is relatively long (~100ms) due to a fortuitous coincidence of the singlet and triplet scattering lengths

P. Julienne, et al., Phys. Rev.Lett. **78**, 1880 (1997)

— long enough for coherent spin dynamics to be observed.

— too short for the equilibrium spin state to be achieved (a few seconds required).

- The small energy scale (~0.1nK) of the spin-singlet pair term requires a very low magnetic field, but then the system suffers stray ac magnetic fields.

Our Proposal

Whether the ground state is antiferromagnetic or cyclic can be determined by the sign of the spin-singlet pair energy.

$$\mathcal{E} \equiv \frac{E}{N} = q \sum_{m=-2}^{2} m^2 \left|\zeta_m\right|^2 + \frac{\tilde{c}_0}{2} + \frac{\tilde{c}_1}{2} f^2 + \frac{\tilde{c}_2}{2} \left|a_{00}\right|^2$$

The value of the singlet pair energy can be determined from the initial spin dynamics.

H.Saito and M.Ueda, cond-mat / 0506520

Case of $|q| < \widetilde{c}_2/10$

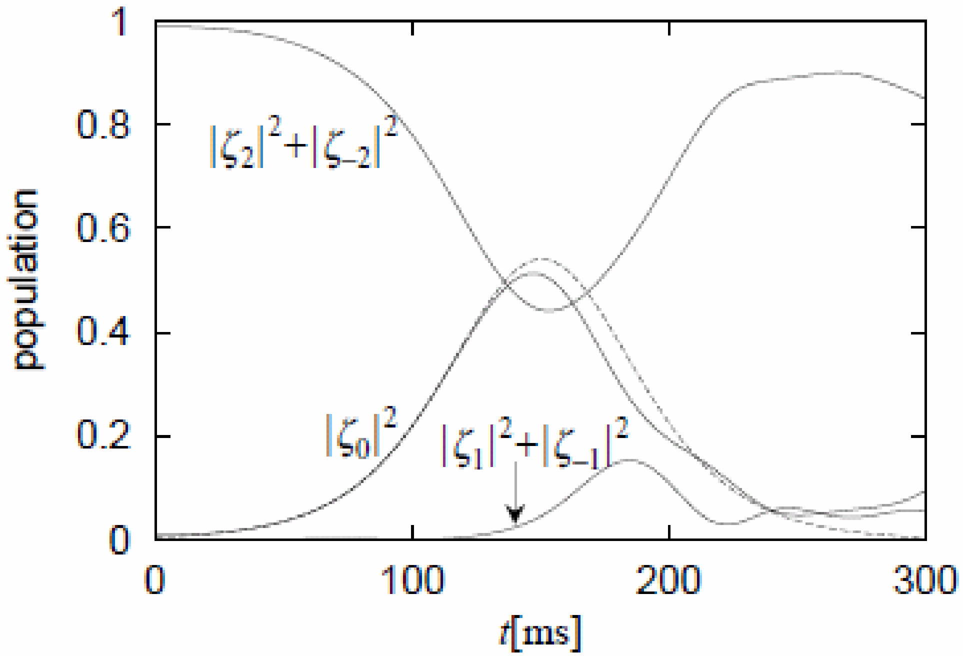

FIG. 4: Time evolution of the spin populations with a magnetic field of 100 mG. The other parameters are the same as in Fig. 2 (a). The initial state is given by $\zeta_0 = \sqrt{0.009}$, $\zeta_{\pm 1} = \sqrt{0.001}$, $\zeta_2 = -\zeta_{-2} = \sqrt{0.99}$. The dashed curve is drawn according to Eq. (41).

Summary

$f = 1$

^{87}Rb ferromagnetism 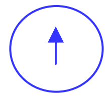

^{23}Na antiferromagnetism 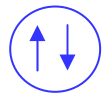 ➨ 2nd phase transition at $T_c \sim \sqrt{N}\,\dfrac{\Delta\varepsilon}{k_B}$

$f = 2$

^{87}Rb AFM or cyclic? 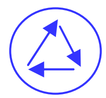 ➨ AFM phase shows Meissner effect.

spin-exchange dynamics
as a sensitive probe of c_2.

Ferromagnetism under spin conservation

1D : staggered magnetic domains
helical structure

2D : concentric ring structure